Mutation-driven modulation of GPCR pharmacology in cancer: insights from adenosine and serotonin receptors

Feng, C.

Chapter 6

The effect of cancer-associated mutations on ligand binding and receptor function – a case for the 5-HT_{2C} receptor

Chenlin Feng, Rongfang Liu, Reno Brooks, Xuesong Wang, Willem Jespers,
Marina Gorostiola González, Gerard J.P. van Westen, Erik H.J. Danen, Laura H. Heitman

Adapted from: *Eur J Pharmacol.* 2024 Dec 15; 985:177081

Abstract

The serotonin 5-HT_{2C} receptor is a G protein-coupled receptor (GPCR) mainly expressed in the central nervous system. Besides regulating mood, appetite, and reproductive behavior, it has been identified as a potential target for cancer treatment. In this study, we aimed to investigate the effects of cancer patient-derived 5-HT_{2C} receptor mutations on ligand binding and receptor functionality. By filtering the sequencing data from the Genomic Data Commons data portal (GDC), we selected 12 mutations from multiple cancer types. We found that the affinity of the endogenous agonist serotonin (5-HT) and inverse agonist mesulergine were both drastically decreased by mutations $L209H^{ECL2}$ and $F328S^{6.52}$, which are located in the orthosteric binding pocket. In the calcium-flux assay, the potency of 5-HT was decreased at $F328S^{6.52}$, while a trend of increased efficacy was observed. In contrast, 5-HT displayed higher affinity at $E306K^{6.30}$ and $E306A^{6.30}$, while a trend of decreased efficacy was observed. These two mutations may disrupt the conserved ionic interaction between $E^{6.30}$ and $R^{3.50}$, and thus increase the constitutive activity of the receptor. The inhibitory potency of mesulergine was increased at $E306A^{6.30}$ but not $E306K^{6.30}$. Lastly, $P365H^{7.50}$ decreased the expression level of the receptor by more than ten-fold, which prevented further functional analyses. This study shows that cancer-associated mutations of 5-HT_{2C} receptor have diverse effects on ligand binding and function. Such mutations may affect serotonin-mediated signaling in tumor cells as well as treatment strategies targeting this receptor.

1. Introduction

The serotonin 5-HT_{2C} receptor is a class A G protein-coupled receptor that is coupled to G_q/G_{11} G protein [1]. A high density of 5-HT_{2C} receptors are located postsynaptically in the central nervous system [2]. Upon activation by the neurotransmitter serotonin (5-HT), the 5-HT_{2C} receptor was found to regulate several important physiological processes, including feeding, anxiety, mood, and reproductive behavior [3-5]. As such, the 5-HT_{2C} receptor is a potential therapeutic target for obesity, depression, obsessive compulsive disorder, and drug addiction [6-8]. Moreover, serotonin is a local mediator in the gut, and a vasoactive agent in the cardiovascular system, which relates to most side effects of 5-HT_{2C} receptor ligands such as nausea, headache, dizziness and cardiac valvulopathy [9, 10].

Symptoms of depression are observed in over half of cancer patients, and as such selective serotonin reuptake inhibitors (SSRI) are prescribed in up to 20% of these patients as anti-depression medication [11]. Combining 5-HT_{2C} receptor blockade with an SSRI has been reported to reverse the SSRI-induced motor defects and potentiate therapeutic efficacy [12]. Interestingly, several studies have linked serotonin signaling to the promotion of tumor growth and metastasis in various cancer types, including liver cancer [13, 14], pancreatic cancer [15], and breast cancer [16-18]. Indeed, lorcaserin (Belviq), a selective 5-HT_{2C} receptor agonist used as an anti-obesity drug, was withdrawn from the market in 2020, because during a randomized clinical trial it was associated with an increased risk for cancer [19]. Therefore, the 5-HT_{2C} receptor might play a stimulatory role in cancer progression and deserves further research as a therapeutic target for cancer treatment.

For 5-HT_{2C} receptor, crystallography together with mutagenesis analysis have been used to reveal the structural basis of ligand interaction and receptor activity [20, 21]. However, there is a lack of focus on the effects of 5-HT_{2C} receptor mutations in disease, such as cancer. To shed light on the function of a potential cancer-driving gene, it is important to illustrate the mutational frequency and their associated biological consequence [22]. In this study, we explored the cancer sequencing resource from the Genomic Data Commons data portal (GDC), and retrieved in total 128 single-base missense mutations of 5-HT_{2C} receptor (encoded by *HTR2C*) in various cancer types [23]. We selected twelve 5-HT_{2C} receptor mutations, and investigated their effects on agonist and antagonist binding affinity and receptor function. The presented characterization of cancer-associated mutations of 5-HT_{2C} receptor will increase the understanding of their role in cancer progression and treatment.

2. Results

2.1. Selection of Cancer-Associated 5-HT_{2C} Receptor Mutations

From the GDC data portal (version 22.0, as collected by Bongers *et al.*) [23, 24], 128 single-base missense mutations of 5-HT_{2C} receptor were retrieved. These mutations were found to affect 153 cases in cohorts of various cancer types. From the 128 mutations, we selected 12 mutations for further investigation based on the following criteria: mutations located in the orthosteric binding pocket (defined by Peng Y *et al.*, PDB ID: 6BQG, 6BQH) of 5-HT_{2C} receptor (V208M, L209H, V215I, F328S) [21], mutations located in conserved motifs of GPCRs (D151Y, R152W, E306K, E306A, P365H), mutations located at the same residue (E197D and E197K), and the mutation that had the highest frequency of occurrence for 5-HT_{2C} receptor (S167L). To be noted, none of these 12 mutations has been identified as a natural variant (The 1000 Genomes Project

Consortium, as collected by Bongers *et al.*) [24, 25]. The resulting 12 mutations are listed in **Table 6.1** and plotted in the primary structure of 5-HT_{2C} receptor in **Figure 6.1**.

Table 6.1. List of 12 cancer-associated 5-HT_{2C} receptor mutations investigated in this study.

Location	Mutation[a]	Affected cases per cancer type across the GDC[b]	Cancer type
TM4	S167L$^{4.38}$	1 / 179 1 / 428 1 / 470 1 / 512	Pancreatic adenocarcinoma (PAAD) Colon adenocarcinoma (COAD) Skin Cutaneous Melanoma (SKCM) Uterine Corpus Endometrial Carcinoma (UCEC)
ECL2	E197D^{ECL2}	1 / 434 1 / 419	Stomach adenocarcinoma (STAD) Ovarian serous cystadenocarcinoma (OV)
	E197K^{ECL2}	1 / 287 1 / 470	Cervical squamous cell carcinoma (CESC) Skin Cutaneous Melanoma (SKCM)
Orthosteric binding pocket[c]	V208M^{ECL2}	1 / 419 1 / 512	Ovarian serous cystadenocarcinoma (OV) Uterine Corpus Endometrial Carcinoma (UCEC)
	L209H^{ECL2}	1 / 490	Lung squamous cell carcinoma (LUSC)
	V215I$^{5.39}$	1 / 408	Bladder Urothelial Carcinoma (BLCA)
	F328S$^{6.52}$	1 / 512	Uterine Corpus Endometrial Carcinoma (UCEC)
DRY motif	D151Y$^{3.49}$	1 / 512	Uterine Corpus Endometrial Carcinoma (UCEC)
	R152W$^{3.50}$	1 / 428 1 / 434 1 / 490	Colon adenocarcinoma (COAD) Stomach adenocarcinoma (STAD) Lung squamous cell carcinoma (LUSC)
$R^{3.50}$ – $E^{6.30}$ ionic lock	E306K$^{6.30}$	2 / 470	Skin Cutaneous Melanoma (SKCM)
	E306A$^{6.30}$	1 / 374	Glioblastoma multiforme (GBM)
NpxxY motif	P365H$^{7.50}$	1 / 512	Uterine Corpus Endometrial Carcinoma (UCEC)

[a] Mutations are shown in the numbering of 5-HT_{2C} receptor amino acid sequence as well as the Ballesteros and Weinstein numbering in superscript [26].
[b] Data from the GDC data portal (version 22.0, as collected by Bongers *et al.*) [23, 24].
[c] Defined by Peng Y *et al.*, PDB ID: 6BQG, 6BQH [21].

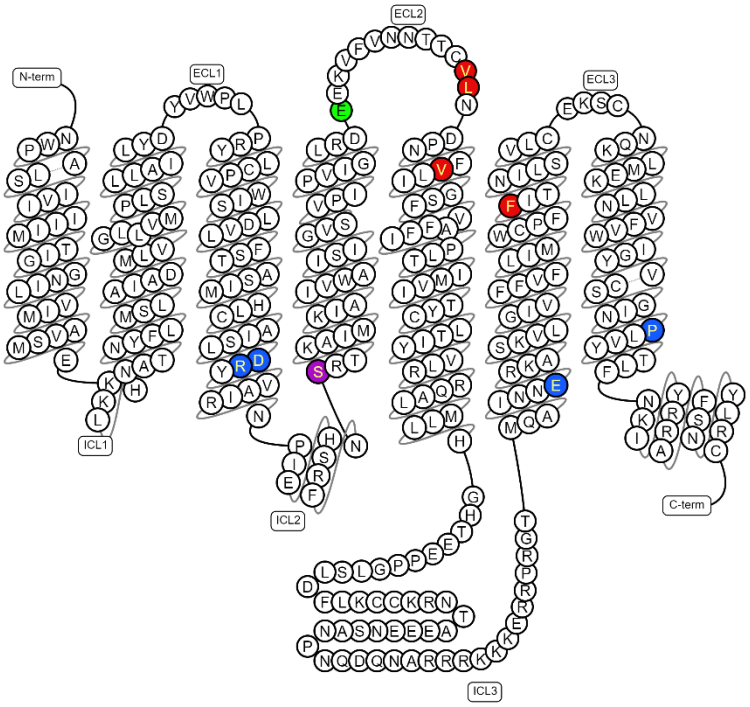

Figure 6.1. Snake-plot showing the primary structure of wild-type human 5-HT$_{2C}$ receptor. Red: cancer-associated mutations in the orthosteric binding pocket (as defined by Peng Y *et al.* [21]); Blue: cancer-associated mutations in conserved motifs within the family of GPCRs; Green: two mutations at the same residue; Purple: mutation with the highest frequency for 5-HT$_{2C}$ receptor in GDC.

2.2. Quantification of Expression Level and Ligand Binding Affinity for Wild-type and Mutant 5-HT$_{2C}$ receptors.

To reveal the effect of the mutations on receptor expression and ligand binding affinity at 5-HT$_{2C}$ receptor, radioligand displacement experiments were performed using [^{3}H]mesulergine and HEK293T cell membranes transiently transfected with wild-type or mutant 5-HT$_{2C}$ receptors. First, receptor expression levels were obtained from radioligand homologous displacement assays and presented as B_{max} values. As shown in **Table 6.2**, six mutants displayed significantly lower expression levels compared to the wild-type 5-HT$_{2C}$ receptor (B_{max} = 5.24 pmol/mg), i.e., S167L (2.28 pmol/mg), E197K (2.76 pmol/mg), L209H (1.38 pmol/mg), F328S (1.53 pmol/mg), D151Y (3.04 pmol/mg), and P365H (0.50 pmol/mg). The other six mutants (E197D, V208M, V215I, R152W, E306K and E306A) displayed expression levels similar to that of the wild-type receptor ($p > 0.05$, ordinary one-way ANOVA).

The affinity of inverse agonist mesulergine was also determined from radioligand homologous displacement assays. K_D values of mesulergine at 5-HT$_{2C}$ receptors are listed in **Table 6.2**. Compared to the wild-type 5-HT$_{2C}$ receptor (K_D = 0.60 nM; **Figure 6.2A**), mesulergine bound to three mutants with significantly lower affinity, i.e. L209H (K_D = 18.6 nM, **Figure 6.2B**), E306K (K_D = 1.51 nM, **Figure 6.2C**) and F328S (K_D = 11.2 nM, **Figure 6.2D**). The K_D values for the other nine mutants were not significantly different from wild-type, indicating that these mutations did not change the binding affinity of mesulergine ($p > 0.05$, ordinary one-way ANOVA).

The binding affinities of endogenous agonist 5-HT (K_i) at the wild-type and mutant 5-HT$_{2C}$ receptors were determined with radioligand heterologous displacement assays. As shown in

Figure 6.3B and **Table 6.2**, L209H (K_i = 204.2 nM), F328S (K_i = 616.6 nM), D151Y (K_i = 64.6 nM), and P365H (K_i = 57.5 nM) significantly decreased the affinity of 5-HT compared to wild-type 5-HT_{2C} receptor (K_i = 21.9 nM). In contrast, E306K (K_i = 1.7 nM) and E306A (K_i = 1.2 nM) significantly increased the affinity of 5-HT by more than 10-fold. The other six mutations did not affect the affinity of 5-HT significantly (**Figure 6.3A**, **Table 6.2**).

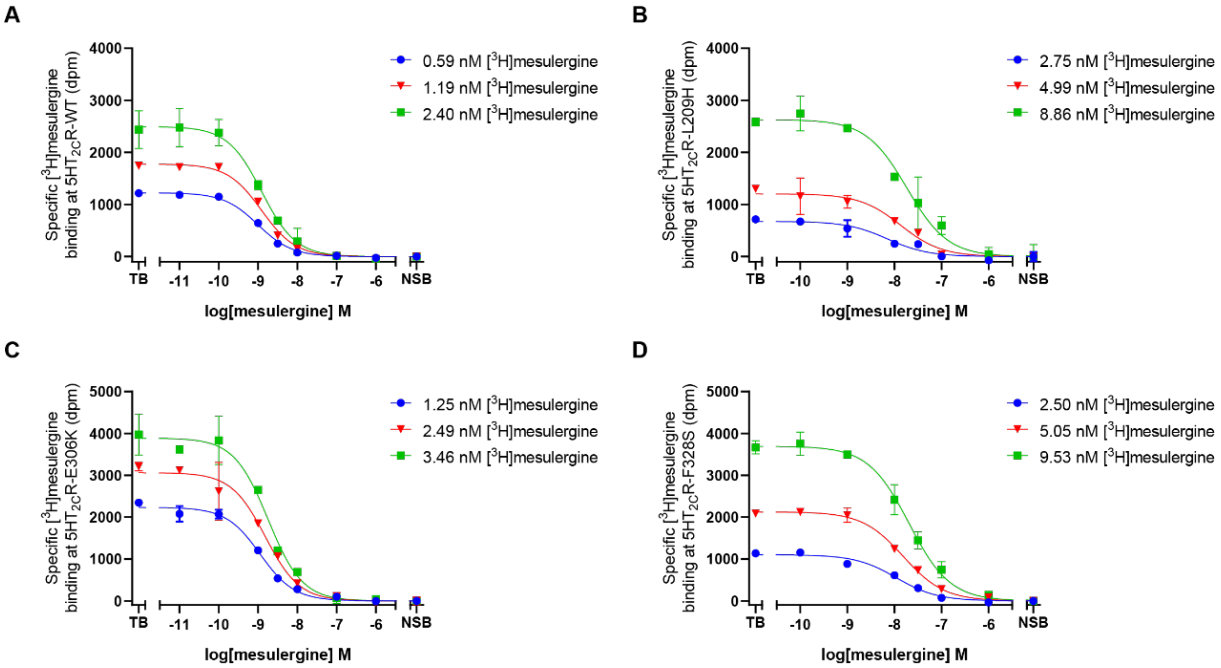

Figure 6.2. Homologous displacement of three concentrations of [^{3}H]mesulergine by increasing concentrations of mesulergine at 5-HT_{2C}R-WT (**A**), 5-HT_{2C}R-L209H (**B**), 5-HT_{2C}R-E306K (**C**) and 5-HT_{2C}R-F328S (**D**). Curves for the other nine mutations are not shown. Note that different concentrations of membranes were used, i.e. 5-HT_{2C}R-WT (3 µg), 5-HT_{2C}R-L209H (30 µg), 5-HT_{2C}R-E306K (5 µg) and 5-HT_{2C}R-F328S (30 µg) to yield similar assay windows. Total binding (TB) was determined with vehicle (1% DMSO in assay buffer), and non-specific binding (NSB) was determined in the presence of 10 µM 5-HT_{2C} receptor agonist lorcaserin. Data are shown as mean ± SD of representative curves from one experiment performed in duplicate.

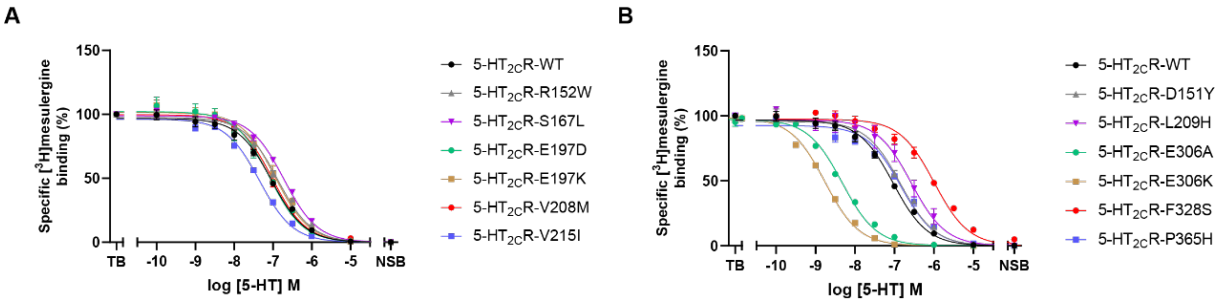

Figure 6.3. Displacement of [^{3}H]mesulergine by increasing concentrations of 5-HT at wild-type and mutant 5-HT_{2C} receptors. (**A**) Mutant 5-HT_{2C} receptors with no significantly different affinity of 5-HT compared to wild-type receptor. (**B**) Mutant 5-HT_{2C} receptors with significantly higher or lower affinity of 5-HT compared to wild-type receptor. Total binding (TB) was determined with vehicle (1% DMSO in assay buffer), and non-specific binding (NSB) was determined with the presence of 10 µM 5-HT_{2C} receptor agonist lorcaserin. Data are shown as mean ± SEM of at least three independent experiments each performed in duplicate.

Table 6.2. Affinity values of endogenous agonist 5-HT (K_i) and inverse agonist mesulergine (K_D) at the wild-type (WT) and mutant 5-HT_{2C} receptors and their expression level (B_{max}).

Mutant	mesulergine pK_D [a] (K_D in nM)	5-HT pK_i [b] (K_i in nM)	B_{max} [a] (pmol/mg)
WT	9.22 ± 0.08 (0.60)	7.66 ± 0.02 (21.9)	5.24 ± 0.45
S167L$^{4.38}$	9.29 ± 0.01 (0.51)	7.41 ± 0.05 (38.9)	2.28 ± 0.04****
E197D^{ECL2}	9.18 ± 0.06 (0.66)	7.34 ± 0.12 (45.7)	4.61 ± 0.38
E197K^{ECL2}	9.22 ± 0.06 (0.60)	7.33 ± 0.07 (46.8)	2.76 ± 0.15****
V208M^{ECL2}	9.11 ± 0.03 (0.78)	7.55 ± 0.05 (28.2)	5.72 ± 0.17
L209H^{ECL2}	7.73 ± 0.07**** (18.6)	6.69 ± 0.11**** (204.2)	1.38 ± 0.15****
V215I$^{5.39}$	9.13 ± 0.07 (0.74)	7.78 ± 0.03 (16.6)	6.10 ± 0.19
F328S$^{6.52}$	7.95 ± 0.06**** (11.2)	6.21 ± 0.04*** (616.6)	1.53 ± 0.09****
D151Y$^{3.49}$	9.08 ± 0.05 (0.83)	7.19 ± 0.03* (64.6)	3.04 ± 0.25****
R152W$^{3.50}$	9.15 ± 0.03 (0.71)	7.48 ± 0.04 (33.1)	5.46 ± 0.10
E306K$^{6.30}$	8.82 ± 0.10** (1.51)	8.78 ± 0.12**** (1.7)	5.28 ± 0.46
E306A$^{6.30}$	9.10 ± 0.06 (0.79)	8.92 ± 0.04**** (1.2)	4.20 ± 0.35
P365H$^{7.50}$	9.22 ± 0.04 (0.60)	7.24 ± 0.04* (57.5)	0.50 ± 0.03****

[a] pK_D and B_{max} were determined by homologous displacement assays, where three concentrations of [^{3}H]mesulergine were displaced by increasing concentrations of mesulergine. [b] pK_i values were determined by heterologous displacement assays, where [^{3}H]mesulergine was displaced by increasing concentrations of 5-HT. Data are represented as Mean ± SEM of at least three independent experiments each performed in duplicate. (Significant difference from wild-type is shown as * P <0.05, ** P <0.01, *** P <0.001, **** P <0.0001, ordinary one-way ANOVA with Dunnett's multiple comparisons tests.)

2.3. Functional Characterization of Cancer-Associated Mutations of 5-HT_{2C} receptor in Calcium-flux Assay

To investigate the effects of cancer-associated 5-HT_{2C} mutations on receptor functionality, calcium-flux assays were performed as an indicator of G_q-coupled receptor activation, i.e. the predominant signaling pathway for this receptor. Initial experiments were conducted with transiently transfected HEK293T cells, which resulted in very small calcium responses (data not shown). As this indicated that HEK293T was not an optimal cellular background for the calcium-flux assay, a switch to U2OS cells transiently transfected with wild-type or mutant 5-HT_{2C} receptors was made. Mutations causing over 3-fold change in the affinity of 5-HT or mesulergine (**Table 6.2**) were selected for functional characterization, i.e. L209H, E306A, E306K and F328S. Moreover, S167L was included as it has the highest frequency amongst all 5-HT_{2C} mutations reported in the GDC (**Table 6.1**).

Firstly, expression levels were determined for wild-type and these five mutants. As such, ELISA was performed on U2OS cells after transfection, which indicated that all five mutants had similar expression levels compared to wild-type receptor (**Figure 6.4A**). Secondly, receptor activation was determined after stimulation with increasing concentrations of 5-HT at the wild-type 5-HT_{2C} receptor, which resulted in an increased signal from the fluorescent Ca^{2+} dye (**Figure 6.4**B). The shape of the curve indicated that intracellular Ca^{2+} levels drastically increased upon agonist addition, reached a peak within 20-40 seconds, and gradually decreased towards baseline afterwards. The 5-HT induced response was dose-dependent and resulted in a potency (pEC_{50}) of 9.16 ± 0.65 for wild-type 5-HT_{2C} receptor (**Figure 6.4C**, **Table 6.3**). Comparing the concentration-response curves among wild-type and mutant 5-HT_{2C} receptors, we found that 5-HT displayed significantly lower potency at F328S (pEC_{50} = 7.68 ± 0.20). There was a reproducible trend towards lower potency at L209H (pEC_{50} = 8.44 ± 0.30), but this was

not significant (P > 0.05, ordinary one-way ANOVAs with Dunnett's multiple comparisons test). We also observed a trend of higher efficacy of 5-HT at F328S (E_{max}% = 269 ± 70) and L209H (E_{max}% = 146 ± 67) comparing to wild-type receptor (E_{max}% = 100 ± 26), albeit not significant. On the contrary, there was a reproducible trend towards higher potency but lower efficacy of 5-HT at E306A (pEC_{50} = 10.25 ± 0.13, E_{max}% = 63 ± 3) and E306K (pEC_{50} = 9.79 ± 0.25, E_{max}% = 60 ± 24), albeit not significant. S132L did not alter the potency (pEC_{50} = 9.21 ± 0.43) or efficacy (E_{max}% = 126 ± 46) of 5-HT.

The inhibition of wild-type and mutant 5-HT_{2C} receptors was characterized by treating the cells with a submaximal concentration of 5-HT (EC_{80}) and increasing concentrations of mesulergine in the calcium-flux assay. The inhibitory potency of mesulergine (pIC_{50}) was obtained from concentration-response curves as shown in **Figure 6.4D** and **Table 6.3**. Compared to wild-type receptor (pIC_{50} = 6.80 ± 0.07), the potency of mesulergine was significantly higher at E306A (pIC_{50} = 7.45 ± 0.09) and similar at the other four mutants (pIC_{50} = 6.88 ± 0.14 for S167L, pIC_{50} = 6.45 ± 0.08 for L209H, pIC_{50} = 6.89 ± 0.08 for E306K, pIC_{50} = 6.91 ± 0.13 for F328S).

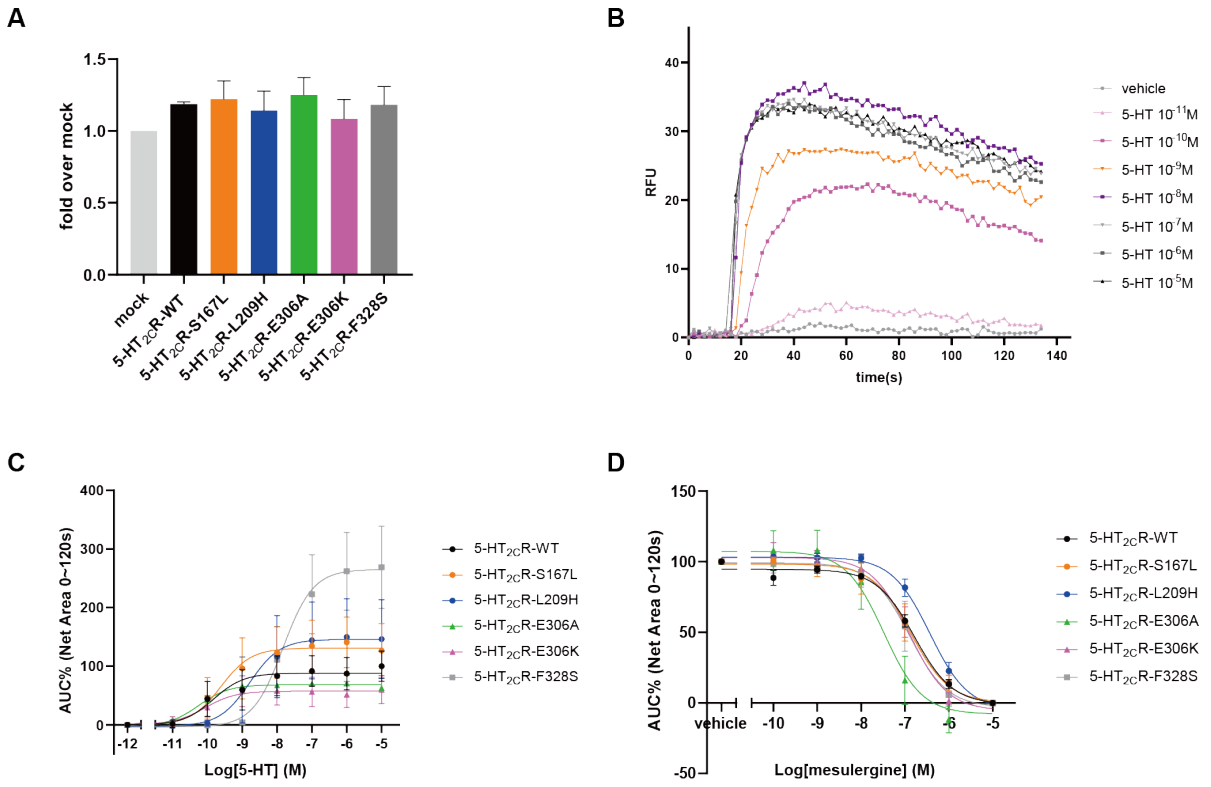

Figure 6.4. Functional characterization of wild-type (WT) and mutant 5-HT_{2C} receptors in transiently transfected U2OS cells, using a calcium-flux assay. (**A**) Expression level of transiently transfected WT and mutant 5-HT_{2C} receptors on U2OS cells, measured by enzyme-linked immunosorbent assay, normalized to mock transfected cells. Data are shown as mean ± SD of two independent experiments performed in quintuplicate. (**B**) Representative graph of baseline- corrected relative fluorescent unit (RFU) after stimulation with increasing concentrations of 5-HT at the WT 5-HT_{2C} receptor. (**C**) Concentration-response curves of 5-HT for WT and five mutant 5-HT_{2C} receptors derived from area under curve within 120 seconds minutes after agonist addition. The response to vehicle was set at 0%, while the response to 10μM 5-HT at the WT 5-HT_{2C} receptor was set at 100%. Data are shown as mean ± SEM of four independent experiments each performed in duplicate. (**D**) Concentration-response curves of mesulergine for WT and five mutant 5-HT_{2C} receptors derived from area under curve within 120 seconds after co-treatment with 5-HT (EC_{80}) and mesulergine. Response to EC_{80} of 5-HT with vehicle was normalized to 100%, and response to EC_{80} of 5-HT with 10 μM mesulergine was set to 0%. Data are shown as mean ± SEM of four independent experiments each performed in duplicate.

Table 6.3. Potency and efficacy of agonist 5-HT and inhibitory potency of inverse agonist mesulergine at the wild-type (WT) and mutant 5-HT_{2C} receptors, determined by calcium-flux assays performed with transiently transfected U2OS cells.

Mutant	Potency of 5-HT pEC_{50} [a]	Efficacy of 5-HT E_{max} (%) [a]	Potency of mesulergine pIC_{50} [b]
WT	9.16 ± 0.65	100 ± 26	6.80 ± 0.07
$S167L^{4.38}$	9.21 ± 0.43	126 ± 46	6.88 ± 0.14
$L209H^{ECL2}$	8.44 ± 0.30	146 ± 67	6.45 ± 0.08
$E306A^{6.30}$	10.25 ± 0.13	63 ± 3	7.45 ± 0.09***
$E306K^{6.30}$	9.79 ± 0.25	60 ± 24	6.89 ± 0.08
$F328S^{6.52}$	7.68 ± 0.20*	269 ± 70	6.91 ± 0.13

[a] Log potency (pEC_{50}) and efficacy (E_{max} %) of 5-HT were calculated from concentration-response curves derived from the area under the curve of RFU changes within 120s after stimulation. [b] Cells were treated with EC_{80} of 5-HT and increasing concentrations of mesulergine at the same time. The inhibitory potency of mesulergine (pIC_{50}) was calculated from concentration-response curves derived from the area under the curve of RFU changes within 120s after compound treatment. Data are represented as mean ± SEM of four independent experiments performed in duplicate. (Significant difference from the wild-type receptor is shown as * $p < 0.05$, ** $p < 0.01$, *** $p < 0.001$; ordinary one-way ANOVAs with Dunnett's multiple comparisons tests.)

3. Discussion

As potential drug targets, attention has been given to the role of serotonin receptors, including the 5-HT_{2C} receptor, in cancer development [27, 28], whereas without much focus on mutants. Hence, in the present study we have investigated a selection of 12 cancer-associated 5-HT_{2C} receptor mutations and found that they are diversely affected. This includes an altered receptor expression level, altered ligand binding affinity, and/or altered receptor functioning. Either of these effects could possibly lead to dysregulation of the downstream signaling pathways and ultimately influence cellular responses to agonists and antagonists targeting this GPCR. In the following paragraphs, we will discuss the structural basis behind these mutation-induced effects and their potential outcomes.

3.1. Cancer-associated mutations affect 5-HT_{2C} receptor expression

Compared to the wild-type 5-HT_{2C} receptor, six mutants had a similar expression level, while mutant $S167L^{4.38}$, $E197K^{ECL2}$, $D151Y^{3.49}$, $L209H^{ECL2}$, $F328S^{6.52}$ had two to four-fold lower expression levels (**Table 6.2**). Notably, mutation $P365H^{7.50}$, located in the highly conserved NPxxY motif, decreased the expression of 5-HT_{2C} receptor by more than ten-fold. The NPxxY motif has been found important for GPCR activation, β-arrestin recruitment and receptor internalization [29, 30]. Earlier research by Prioleau *et al.* reported that mutation $Y368F^{7.53}$ in the same motif of the 5-HT_{2C} receptor caused a two-fold lower receptor expression level [31]. The B_{max} values obtained by Cassandra *et al.* were from a homologous displacement assay using the same radioligand, but a different cell line (COS-1), which might explain a difference in the degree of impact. Thus, our study further establishes that mutations in the NPxxY motif affect receptor expression, most probably due to dysregulated receptor trafficking.

We also performed ELISA assays in transiently transfected U2OS cells for wild-type 5-HT_{2C} receptor and five mutants. Based on ELISA results, the mutants showed expression levels not significantly different from the wild-type receptor (**Figure 6.4A**). However, among these five mutants, the B_{max} values of $S167L^{4.38}$, $L209H^{ECL2}$, $F328S^{6.52}$ obtained from homologous displacement experiments in HEK293T cells indicated that they had lower expression level. The

inconsistency of two different assays might be caused by the relatively low sensitivity of ELISA for protein detection (i.e. qualitative assessment), whereas the homologous displacement assay yields quantitative data. In addition, cell context dependency, i.e. HEK293T vs. U2OS cells, might also explain differences in receptor expression [32].

3.2. Cancer-associated mutations affect ligand binding at 5-HT$_{2C}$ receptor

This study shows that mutations L209H^{ECL2} and F328S$^{6.52}$ decreased the affinity of both 5-HT and mesulergine for the receptor by more than ten-fold (**Figure 6.2 & 6.3, Table 6.2**). Both mutations are located in the orthosteric binding pocket of 5-HT$_{2C}$ receptor. Where based on the crystal structure of 5-HT$_{2C}$ receptor bound with agonist ergotamine (PDB: 6BQG) and inverse agonist ritanserin (PDB: 6BQH), L209^{ECL2} forms a hydrogen bond with the carbonyl of ergotamine, and F328$^{6.52}$ forms an edge-to-face aromatic interaction with the backbone phenyl ring of both ergotamine and ritanserin [21]. Although the 5-HT or mesulergine bound structures of 5-HT$_{2C}$ receptor have not been solved, for mutation L209^{ECL2}, the substitution of leucine with the positively charged histidine at ECL2 could hinder ligand entry and thus decrease the affinity of 5-HT and mesulergine. Interestingly, mutations at the adjacent residues V208M^{ECL2} and V215I$^{5.39}$ did not affect the affinity of 5-HT or mesulergine, indicating that the substitution of valine with similarly hydrophobic and sized methionine or isoleucine had little influence on ligand binding. On the other hand, the F328S$^{6.52}$ mutation could disrupt the potential aromatic interaction with 5-HT and mesulergine, and thereby significantly decreases their binding affinity to the receptor.

We observed that mutations outside of the binding pocket of the 5-HT$_{2C}$ receptor can also have an influence on ligand binding. For example, D151Y$^{3.49}$ and P365H$^{7.50}$ moderately decreased the affinity of 5-HT by approximately three-fold. These two mutations are located in the conserved DRY motif and NPxxY motif respectively, so their impact on agonist binding affinity might be an indirect consequence of their influence on receptor conformation. Specifically, mutations rendering the receptor towards an inactive state would lead to lower affinity for agonists [33]. On the contrary, E306A$^{6.30}$ as well as E306K$^{6.30}$ significantly increased the affinity of the agonist 5-HT by more than ten-fold, and E306K$^{6.30}$ also decreased the affinity of inverse agonist mesulergine, indicative that these mutations bring the receptor towards a more active conformation. In class A GPCRs, it has been shown that a salt bridge formed by conserved D/E$^{6.30}$ and R$^{3.50}$ acts as an ionic lock, which holds the cytoplasmic ends of TM3 and TM6 in close vicinity and restrains the receptor in an inactive state [34]. Substitution of negatively charged glutamic acid with positively charged lysine or non-charged alanine would therefore abolish this ionic lock and shift the 5-HT$_{2C}$ receptor towards an active state, which is consistent with our results. However, this ionic lock could also be disrupted by the R152W$^{3.50}$ mutation, i.e. the positively charged arginine is substituted by a non-charged (and bulkier) tryptophan, but the affinity of agonist 5-HT was not increased accordingly. A similar phenomenon has been observed at the histamine H4 receptor, showing that this ionic lock is not generally essential for all class A GPCRs and that alternative interactions may play a role in the R$^{3.50}$ mutated receptor [35].

3.3. Cancer-associated mutations affect the functioning of 5-HT$_{2C}$ receptor

For the investigated wild-type and five mutant receptors (**Figure 6.4, Table 6.3**), we found that 5-HT displayed a significantly lower potency at F328S$^{6.52}$, correlated with the drastic decrease in affinity. Comparing to F328S$^{6.52}$, the affinity of 5-HT was less decreased by L209H^{ECL2}, which could explain the non-significant trend towards decreased potency at L209H^{ECL2}. Interestingly,

we also observed reproducible albeit non-significant trend of increased efficacy (E_{max}%) of 5-HT at these two mutants. These seemingly counterintuitive results indicate that although ligand binding is compromised, a higher coupling efficiency of the receptor with the downstream signaling proteins such as the G_q protein is yielded. The structural basis behind this effect needs further investigation. In addition, we found a non-significant trend of higher potency but lower efficacy of 5-HT at E306A$^{6.30}$ and E306K$^{6.30}$ comparing to the wild-type receptor, which further supported that the receptor was shifted towards the active state and rendered higher constitutive activity by mutations at E306$^{6.30}$. As calcium-flux assays typically can not detect constitutive activity of GPCRs, the assumption that the constitutive activity of these two mutant receptors is increased should be confirmed in another functional assay, such as IP_3 accumulation assays. The 5-HT_{2C} receptor is known for its relatively high constitutive activity [36-38], and 5-HT is systemically present in normal tissue and shown to be elevated in multiple tumors [39]. Thus, it cannot be ruled out that the 5-HT_{2C} receptor might be activated by circulating 5-HT, and the overall activation level of the receptor would be influenced by both the constitutive activity and surrounding levels of 5-HT.

With respect to cancer treatment, 5-HT_{2C} antagonists are potential drug candidates, and whether a mutant 5-HT_{2C} receptor can be successfully inhibited deserves more attention as mutations are one of the leading causes of drug resistance [40]. As shown in **Figure 6.4D** and **Table 6.3**, there was a non-significant trend towards decreased potency of mesulergine at L209H^{ECL2}, possibly caused by the decreased affinity of mesulergine. Compared to L209H^{ECL2}, mesulergine displayed around two-fold higher affinity at F328S$^{6.52}$, while 5-HT had three-fold lower affinity. Competition between the agonist and antagonist binding can explain why these two mutations in the orthosteric binding site have an opposite effect on receptor activation vs. inhibition. We have observed a similar phenomenon at another class A GPCR, the adenosine A_{2A} receptor (A_{2A}AR), where mutation V275A$^{7.40}$ increased the affinity of agonist NECA but retained the affinity of antagonist ZM241385, leading to a lower inhibitory potency [41]. For E306A$^{6.30}$ mutant, the affinity of mesulergine was not affected (**Table 6.2**), while a significantly increased potency of mesulergine was observed (**Figure 6.4D, Table 6.3**). This indicates that the agonist-induced activation of this constitutively active mutant can be efficiently inhibited by mesulergine.

Notably, with the highest frequency amongst all 5-HT_{2C} mutations reported in GDC (4 cases out of ~13,000 patients screened), S167L$^{4.38}$ did not show any significant biological or pharmacological consequences. This indicates that S167L$^{4.38}$ most likely represents a passenger mutation in cancer. The identification and characterization of mutational hotspots in GPCRs in specific cancer types would facilitate drug targeting in cancer, and thus raises the call for a larger sample size.

3.4. Conclusions

In this research, we investigated 12 cancer-associated mutations of 5-HT_{2C} receptor and found that they have diverse effects. Firstly, mutations in the orthosteric binding pocket tend to affect ligand binding affinity and thereby their functional activity at the receptor. Secondly, mutations in the conserved motifs can cause a change in receptor conformation, which indirectly impact ligand binding, and they might also influence the constitutive activity of the receptor. Thirdly, the druggability of a mutant receptor was affected by the relative change in affinity of the agonist versus the inverse agonist. These effects on receptor pharmacology may have different consequences for cancer cells with different tissue microenvironments. For example, compared

with to the wild-type 5-HT_{2C} receptor, $L209H^{ECL2}$ and $F328S^{6.52}$ were less easily activated due to a decreased potency for 5-HT, but when high levels of 5-HT are circulating in the surrounding tissues the receptor will be activated to a higher level (increased efficacy). In conclusion, this study provides insights into the effect of cancer-associated 5-HT_{2C} receptor mutations on receptor function and ligand binding, and invites future research to reveal the effects of mutations on cancer growth and metastasis. This will provide further insight in the potential of 5-HT_{2C} targeted cancer treatment, finally facilitating drug discovery and personalized medicine.

4. Materials and Methods

4.1. Chemicals and Reagents

The wild-type human 5-HT_{2C} receptor plasmid pcDNA3.1(+)-FLAG-HTR2C was purchased from GenScript Biotech (Leiden, the Netherlands). Quick Change II Site-Directed Mutagenesis Kit was purchased from Agilent Technologies Netherlands B.V. (Amstelveen, the Netherlands). QIAprep Spin Miniprep kit as well as the QIAGEN plasmid Midi kit were purchased from QIAGEN (Amsterdam, the Netherlands). BCA protein assay reagent was obtained from Fisher Scientific (Landsmeer, the Netherlands). [^{3}H]mesulergine (Specific Activity at t_0 = 81.6 Ci/mmol) was obtained from PerkinElmer (Groningen, the Netherlands). Mesulergine hydrochloride was purchased from Santa Cruz Biotechnology. Lorcaserin was purchased from Adooq Bioscience. Serotonin hydrochloride was purchased from Sigma-Aldrich. Fluo-4 Direct™ calcium assay kit was purchased from Fisher Scientific (Landsmeer, the Netherlands). All other reagents were of analytical grade and obtained from standard commercial sources.

4.2. Site-Directed Mutagenesis

Plasmid DNA of mutant 5-HT_{2C} receptors were constructed by polymerase chain reaction (PCR) using Quick Change II Site-Directed Mutagenesis Kit, and pcDNA3.1(+)-HTR2C with N-terminal FLAG tag as template. Mutagenesis primers for PCR cloning were designed using the online Quickchange primer design tool (Agilent Technologies) and synthesized by Integrated DNA Technologies (Coral-ville, USA). DNA sequences with the corresponding mutations were amplified in supercompetent E. coli (Escherichia coli) cells, purified with QIAprep Spin Miniprep kit, and verified by Sanger sequencing at Leiden Genome Technology Center (Leiden, the Netherlands). After that, correct DNA sequences were further amplified and purified using QIAGEN plasmid Midi kit and used for transfection.

4.3. Cell culture and transfection

Human embryonic kidney 293T (HEK293T) cells were grown in Dulbecco's modified Eagle's medium (high glucose, D6546, Sigma) supplemented with 10% fetal calf serum, 2 mM glutamax, 200 µg/ml penicillin, 200 µg/ml streptomycin, at 37°C and 5% CO_2. Cells were subcultured at a ratio of 1:15 twice a week on 10 cm ø plates. Human bone osteosarcoma epithelial (U2OS) cells were grown in Dulbecco's modified Eagle's medium (high glucose, D6546, Sigma) supplemented with 10% newborn calf serum, 2 mM glutamax, 200 µg/ml penicillin, 200 µg/ml streptomycin, at 37°C and 5% CO_2. Cells were subcultured at a ratio of 1:8 twice a week on 10 cm ø plates.

HEK293T cells were subcultured 24 hours before transfection, and they reached 50%-70% confluency when the transfection was performed, where polyethyleneimine (PEI) method was used [42]. In short, for each 10 cm ø plate, 10 µg plasmid DNA of wild-type or mutant pcDNA3.1(+)-FLAG-HTR2C and 30 µg PEI was separately dissolved in 500 µl OptiMEM, then the

PEI and DNA solutions were mixed to get 1 mL DNA/PEI mixture (1:3 ratio). The mixture was incubated at room temperature for 30 minutes. HEK293T cells was refreshed with 9 mL antibiotic free medium and then applied with 1mL DNA/PEI mixture. Cells were incubated at 37°C and 5% CO_2 for 24 hours and refreshed with culture medium. After that, cells were left to grow for another 24 hours before preparation of cell membranes expressing (mutant) 5-HT_{2C} receptor.

For U2OS cells, a similar transfection method was used, except that 1mL DNA/PEI mixture (1:3 ratio) containing 5 μg DNA and 15 μg PEI was applied to each 10 cm ø plate. And 24 hours after transfection, the cells were digested and seeded for use in the calcium-flux assay, as described in section 4.7.

4.4. Membrane preparation

Preparation of HEK293T cell membranes over-expressing 5-HT_{2C} receptors for radioligand binding assays were performed as previously described with some modifications [41]. Cells were detached by scraping into PBS, and cell pellets from twenty 10 cm ø plates were collected by centrifugation at 1000 rpm for 10 min to remove PBS, and re-suspended in 15 mL ice-cold Tris-HCl buffer (50 mM, PH=7.4). Cell suspension was homogenized with an UltraThurrax homogenizer (Heidolph Instruments, Schwabach, Germany). The homogenized suspensions were centrifuged at 100,000 × g for 20 min at 4°C, and re-suspended in 8 mL Tris-HCl buffer. The homogenization-centrifugation cycle was repeated. After that, membranes from twenty 10 cm ø plates were suspended in 2 mL ice-cold assay buffer (50 mM Tris-HCl, 10 mM $MgCl_2$, 1 mM EDTA, 0.1% BSA) and homogenized again. Membranes were aliquoted and stored at -80°C. Total protein concentration of the HEK293T cell membranes were determined using the BCA method [43].

4.5. Radioligand Homologous and Heterologous Displacement Assays

In radioligand displacement experiments, each reaction unit contained three components mixed in a total volume of 100 μl assay buffer, which were HEK293T membrane suspension, compound of interest, and radioligand. The assay buffer contains 50 mM Tris-HCl, 10 mM $MgCl_2$, 1 mM EDTA, and 0.1% BSA as recommended by Perkin Elmer (Groningen, the Netherlands). For membrane suspension of each mutant, 2 μg ~ 30 μg protein were used to obtain a specific binding window with 2 nM [^{3}H]mesulergine of approximately 1300 dpm. In the homologous displacement assay, increasing concentrations (10^{-11} M to 10^{-6} M) of unlabeled mesulergine were applied to displace the binding of [^{3}H]mesulergine at three different concentrations, which were distributed around the estimated K_D of mesulergine at wild-type or corresponding mutant 5-HT_{2C} receptor. In the heterologous displacement assay, increasing concentrations (10^{-10} M to 10^{-5} M) of 5-HT were applied to displace the binding of 2 nM [^{3}H]mesulergine. For both assays, non-specific binding (NSB) was determined with the presence of 10 μM 5-HT_{2C} receptor specific agonist lorcaserin, and total binding (TB) was determined in presence of vehicle (1% DMSO in assay buffer). The mixtures were incubated at 25°C for 4 hours while shaking at 400 rpm. Incubation was terminated by rapid vacuum filtration to separate the bound and free radioligand through 96-well GF/C filter (presoaked with 0.5% w/v PEI for 1 hour) using Filtermate-harvester (PerkinElmer, Groningen, the Netherlands). Filters were washed ten times with ice-cold wash buffer (50 mM Tris-HCl, PH = 7.4) before drying at 55°C oven for 30 minutes. To measure the membrane-bound radioactivity, 25 ul MicroScint™-20 cocktail was added to each well, and the filter was measured by MicroBeta^2 Microplate Counter (PerkinElmer, Groningen, the Netherlands).

4.6. Enzyme-linked Immunosorbent assay (ELISA)

ELISA was performed to determine the expression levels of wild-type or mutant 5-HT_{2C} receptors on U2OS cells, where cells transfected with pcDNA3.1 vector plasmid were used as mock control. 24 hours after transfection, cells were detached with trypsol (0.25% w/v in PBS containing 4.4 mM EDTA) and re-suspended in culture medium. Cell suspensions were diluted to 1 x 10^6/mL of live cell count, and seeded in 96-well plate at a density of 1 × 10^5 cells/well (5 wells for each sample). Cells were incubated at 37°C and 5% CO_2 for 24 hours, washed with PBS and fixed with 100 µl/well 4% formaldehyde for 10 minutes. Cells were then washed twice with TBS (20 mM Tris-HCl,150 mM NaCl (pH 7.5)), and treated with 100 µl/well blocking buffer (2% w/v bovine serum albumin in TBST) for 30 minutes at room temperature. After that, blocking buffer was removed and cells were incubated in 100 µl/well primary antibody (mouse anti-FLAG monoclonal antibody, Sigma F3165, 1:4000) for 2 hours at room temperature while shaking at 300rpm. Next, the primary antibody was removed and cells were washed with TBST (TBS with 0.1% Tween-20) three times, incubated in 100 µl/well secondary antibody (goat anti-mouse IgG HRP-conjugated, Jackson ImmunoResearch Laboratories 115-035-003, 1:20000) for 1 hour at room temperature while shaking. After removal of the secondary antibody, cells were washed three times with TBS. Next, cells were treated with 100 µl/well 3, 3', 5, 5'-tetramethylbenzidine (TMB, Sigma T0440) for 5 minutes in dark, then the reaction was stopped by addition of 100 µl/well 1 M H_3PO_4 solution. Immediately after that, the absorbance was measured at 450 nm using EnVision™ microplate reader (Menlo Park, CA, USA).

4.7. Calcium-flux Assay

To functionally characterize the cancer-associated mutations, calcium-flux assays were performed with transiently transfected U2OS cells over-expressing wild-type or mutant 5-HT_{2C} receptors. 24 hours after transfection, the cells were washed with PBS, detached with trypsol (0.25% w/v in PBS containing 4.4 mM EDTA) and suspended in culture medium. Cell suspensions were centrifuged at 1000 rpm for 5 min. After that, supernatant was removed and cells were re-suspended in modified culture medium, i.e. culture medium was supplemented with 5 mM sodium butyrate to enhance receptor expression, and 10% newborn calf serum was replaced by 10% dialyzed fetal calf serum to eliminate 5-HT from the medium. Cell suspension was adjusted to 4 x 10^5/mL of live cell count, and seeded in 96-well plate (Corning CLS3603, black wall, clear bottom) at a density of 4 × 10^4 cells/well in duplicate. Cells were left to grow at 37°C and 5% CO_2 for 20 hours before the assay was conducted.

On the day of the assay, medium was carefully removed from the plate, and 95 µl dye loading solution was added to each well. The dye loading solution was prepared in assay buffer (1 x HBSS, 20 mM HEPES) as instructed in the manual of Fluo-4 Direct™ calcium assay kit (Thermofisher F10471). Cells were then incubated in darkness at 37°C for 1 hour, and loaded into the reading chamber of Flexstation 3 multi-mode plate reader (Molecular Devices, CA, USA). Fluorescent intensity (excitation: 494 nM, emission: 516 nM) was measured every 2 seconds within the first 15 seconds as baseline. Subsequently, cells were stimulated with 5 µl agonist 5-HT (final concentration from 10^{-11} M to 10^{-5} M) or vehicle control (final concentration of 0.1% DMSO). Immediately after that, the fluorescent intensity was measured every 2 seconds for 120 seconds.

To characterize the inhibitory effects of mesulergine at 5-HT_{2C} receptors, the experiments were performed similar as described above. After the baseline measurement, the cells were treated with 5 µl compounds mixture of mesulergine and 5-HT (final concentration of mesulergine

ranged from 10^{-10} M to 10^{-5} M, vehicle as control; final concentration of 5-HT equal to the EC_{80} for each 5-HT_{2C} receptor mutant). After that, the fluorescent intensity was measured every 2 seconds for 120 seconds.

4.8. Data analysis and statistics

All experimental data were analyzed using GraphPad Prism 9.0 (GraphPad Soft-ware Inc., San Diego, CA) and values obtained were means of two to four independent experiments. From radioligand homologous displacement assays, K_D and B_{max} values of [^{3}H]mesulergine were calculated using nonlinear regression curve fitting (Binding-Competitive-One site-Homologous), where three concentrations of [^{3}H]mesulergine were input and K_D was obtained by global fitting. B_{max} values were obtained in "dpm", and converted to pmol/mg using the following equations:

$$\boldsymbol{B_{max}\ (Ci) = \frac{Bmax\ (dpm)}{2.22\ *\ 10^{-12}}}$$

$$\boldsymbol{B_{max}\ (mmol) = B_{max}\ (Ci)/Specific\ activity\ (Ci/mmol)}$$

$$\boldsymbol{Specific\ activity = Specific\ activity\ at\ t_0 *\ 0.5^{\frac{time\ lapse\ since\ prodection\ date}{half\ life\ of\ radio\ label}}}$$

$$\boldsymbol{B_{max}\ (pmol/mg) = \frac{B_{max}\ (mmol)\ *\ 10^9}{Amout\ of\ membrane\ protein\ per\ well\ (mg)}}$$

IC_{50} values of 5-HT obtained from radioligand heterologous displacement assays were calculated by non-linear regression curve fitting using a one-site competitive binding model, where K_D of radioligand were taken from homologous displacement assay for each receptor variant, and K_i of 5-HT were converted from IC_{50} following the Cheng-Prusoff equation [44]:

$$\boldsymbol{K_i = \frac{IC_{50}}{1 + \frac{[Radioligand]}{K_D}}}$$

For calcium-flux assays, relative fluorescent unit (RFU) of each group was corrected by subtracting the baseline, and area under curve (AUC) within 120 seconds upon agonist addition was used to generate the dose-response curves, where the response to vehicle was normalized as 0%, and the response to 10 μM 5-HT at the wild-type 5-HT_{2C} receptor was normalized as 100%. Parameters including EC_{50}, EC_{80} and E_{max} of 5-HT were obtained by analyzing the dose-response curves using nonlinear regression fitting (log(agonist) vs. response (three parameters)), which were used to describe the potency and efficacy of 5-HT stimulation at wild-type or mutant 5-HT_{2C} receptors.

For characterization of receptor inhibition using calcium-flux assays, AUC within 120 seconds upon compounds addition was used to generate the dose-response curves of mesulergine. Response to EC_{80} of 5-HT with vehicle was normalized as 100%, and response to EC_{80} of 5-HT with 10 μM mesulergine was set to 0%. IC_{50} values of mesulergine were obtained using nonlinear regression fitting (log(inhibitor) vs. response (three parameters)).

References

1. Day, M., et al., *Stimulation of 5-HT(2) receptors in prefrontal pyramidal neurons inhibits Ca(v)1.2 L type Ca(2+) currents via a PLCbeta/IP3/calcineurin signaling cascade.* J Neurophysiol, 2002. **87**(5): p. 2490-504.
2. Barnes, N.M. and T. Sharp, *A review of central 5-HT receptors and their function.* Neuropharmacology, 1999. **38**(8): p. 1083-1152.
3. Tecott, L.H., et al., *Eating disorder and epilepsy in mice lacking 5-HT2c serotonin receptors.* Nature, 1995. **374**(6522): p. 542-6.
4. Kimura, A., et al., *Overexpression of 5-HT2C receptors in forebrain leads to elevated anxiety and hypoactivity.* Eur J Neurosci, 2009. **30**(2): p. 299-306.
5. Popova, N.K. and T.G. Amstislavskaya, *5-HT2A and 5-HT2C serotonin receptors differentially modulate mouse sexual arousal and the hypothalamo-pituitary-testicular response to the presence of a female.* Neuroendocrinology, 2002. **76**(1): p. 28-34.
6. Garfield, A.S. and L.K. Heisler, *Pharmacological targeting of the serotonergic system for the treatment of obesity.* J Physiol, 2009. **587**(1): p. 49-60.
7. Martin, J.R., et al., *5-HT2C receptor agonists: pharmacological characteristics and therapeutic potential.* J Pharmacol Exp Ther, 1998. **286**(2): p. 913-24.
8. Palacios, J.M., A. Pazos, and D. Hoyer, *A short history of the 5-HT(2C) receptor: from the choroid plexus to depression, obesity and addiction treatment.* Psychopharmacology (Berl), 2017. **234**(9-10): p. 1395-1418.
9. Martin, C.K., et al., *Lorcaserin, a 5-HT(2C) receptor agonist, reduces body weight by decreasing energy intake without influencing energy expenditure.* J Clin Endocrinol Metab, 2011. **96**(3): p. 837-45.
10. Roth, B.L., *Drugs and valvular heart disease.* N Engl J Med, 2007. **356**(1): p. 6-9.
11. Sanjida, S., et al., *A systematic review and meta-analysis of prescribing practices of antidepressants in cancer patients.* Psychooncology, 2016. **25**(9): p. 1002-16.
12. Demireva, E.Y., et al., *5-HT2C receptor blockade reverses SSRI-associated basal ganglia dysfunction and potentiates therapeutic efficacy.* Molecular Psychiatry, 2020. **25**(12): p. 3304-3321.
13. Fatima, S., et al., *5-Hydroxytryptamine promotes hepatocellular carcinoma proliferation by influencing β-catenin.* Mol Oncol, 2016. **10**(2): p. 195-212.
14. Liang, C., et al., *Serotonin promotes the proliferation of serum-deprived hepatocellular carcinoma cells via upregulation of FOXO3a.* Mol Cancer, 2013. **12**: p. 14.
15. Jiang, S.H., et al., *Increased Serotonin Signaling Contributes to the Warburg Effect in Pancreatic Tumor Cells Under Metabolic Stress and Promotes Growth of Pancreatic Tumors in Mice.* Gastroenterology, 2017. **153**(1): p. 277-291.e19.
16. Ballou, Y., et al., *5-HT serotonin receptors modulate mitogenic signaling and impact tumor cell viability.* Mol Clin Oncol, 2018. **9**(3): p. 243-254.
17. Gautam, J., et al., *Tryptophan hydroxylase 1 and 5-HT 7 receptor preferentially expressed in triple-negative breast cancer promote cancer progression through autocrine serotonin signaling.* Molecular cancer, 2016. **15**: p. 1-14.
18. Gautam, J., Y.K. Bae, and J.A. Kim, *Up-regulation of cathepsin S expression by HSP90 and 5-HT(7) receptor-dependent serotonin signaling correlates with triple negativity of human breast cancer.* Breast Cancer Res Treat, 2017. **161**(1): p. 29-40.
19. Sharretts, J., et al., *Cancer Risk Associated with Lorcaserin — The FDA's Review of the CAMELLIA-TIMI 61 Trial.* New England Journal of Medicine, 2020. **383**(11): p. 1000-1002.
20. Liu, Y., et al., *Mutagenesis Analysis Reveals Distinct Amino Acids of the Human Serotonin 5-HT(2C) Receptor Underlying the Pharmacology of Distinct Ligands.* ACS Chem Neurosci, 2017. **8**(1): p. 28-39.
21. Peng, Y., et al., *5-HT(2C) Receptor Structures Reveal the Structural Basis of GPCR Polypharmacology.* Cell, 2018. **172**(4): p. 719-730.e14.
22. Arang, N. and J.S. Gutkind, *G Protein-Coupled receptors and heterotrimeric G proteins as cancer drivers.* FEBS Lett, 2020. **594**(24): p. 4201-4232.
23. Jensen, M.A., et al., *The NCI Genomic Data Commons as an engine for precision medicine.* Blood, 2017. **130**(4): p. 453-459.

24. Bongers, B.J., et al., *Pan-cancer functional analysis of somatic mutations in G protein-coupled receptors.* Sci Rep, 2022. **12**(1): p. 21534.
25. Consortium, G.P., *A global reference for human genetic variation.* Nature, 2015. **526**(7571): p. 68.
26. Ballesteros, J.A. and H. Weinstein, *Integrated methods for the construction of three-dimensional models and computational probing of structure-function relations in G protein-coupled receptors*, in *Receptor Molecular Biology*, S.C. Sealfon, Editor. 1995, Academic Press. p. 366-428.
27. Balakrishna, P., et al., *Serotonin Pathway in Cancer.* Int J Mol Sci, 2021. **22**(3).
28. Karmakar, S. and G. Lal, *Role of serotonin receptor signaling in cancer cells and anti-tumor immunity.* Theranostics, 2021. **11**(11): p. 5296-5312.
29. Barak, L.S., et al., *The conserved seven-transmembrane sequence NP(X)2,3Y of the G-protein-coupled receptor superfamily regulates multiple properties of the beta 2-adrenergic receptor.* Biochemistry, 1995. **34**(47): p. 15407-14.
30. Schönegge, A.-M., et al., *Evolutionary action and structural basis of the allosteric switch controlling β2AR functional selectivity.* Nature Communications, 2017. **8**(1): p. 2169.
31. Prioleau, C., et al., *Conserved helix 7 tyrosine acts as a multistate conformational switch in the 5HT2C receptor. Identification of a novel "locked-on" phenotype and double revertant mutations.* J Biol Chem, 2002. **277**(39): p. 36577-84.
32. Magalhaes, A.C., H. Dunn, and S.S. Ferguson, *Regulation of GPCR activity, trafficking and localization by GPCR-interacting proteins.* British journal of pharmacology, 2012. **165**(6): p. 1717-1736.
33. Park, P.S., D.T. Lodowski, and K. Palczewski, *Activation of G protein-coupled receptors: beyond two-state models and tertiary conformational changes.* Annu Rev Pharmacol Toxicol, 2008. **48**: p. 107-41.
34. Zhou, Q., et al., *Common activation mechanism of class A GPCRs.* eLife, 2019. **8**: p. e50279.
35. Schneider, E.H., et al., *Impact of the DRY motif and the missing "ionic lock" on constitutive activity and G-protein coupling of the human histamine H4 receptor.* J Pharmacol Exp Ther, 2010. **333**(2): p. 382-92.
36. Teitler, M., K. Herrick-Davis, and A. Purohit, *Constitutive activity of G-protein coupled receptors: emphasis on serotonin receptors.* Curr Top Med Chem, 2002. **2**(6): p. 529-38.
37. Deurwaerdère, P.D., et al., *Constitutive Activity of the Serotonin2C Receptor Inhibits In Vivo Dopamine Release in the Rat Striatum and Nucleus Accumbens.* The Journal of Neuroscience, 2004. **24**(13): p. 3235-3241.
38. Berg, K.A., et al., *Physiological relevance of constitutive activity of 5-HT2A and 5-HT2C receptors.* Trends Pharmacol Sci, 2005. **26**(12): p. 625-30.
39. Ye, D., et al., *The role of 5-HT metabolism in cancer.* Biochim Biophys Acta Rev Cancer, 2021. **1876**(2): p. 188618.
40. Holohan, C., et al., *Cancer drug resistance: an evolving paradigm.* Nature Reviews Cancer, 2013. **13**(10): p. 714-726.
41. Feng, C., et al., *Cancer-Associated Mutations of the Adenosine A(2A) Receptor Have Diverse Influences on Ligand Binding and Receptor Functions.* Molecules, 2022. **27**(15).
42. Longo, P.A., et al., *Transient mammalian cell transfection with polyethylenimine (PEI).* Methods Enzymol, 2013. **529**: p. 227-40.
43. Smith, P.K., et al., *Measurement of protein using bicinchoninic acid.* Anal Biochem, 1985. **150**(1): p. 76-85.
44. Yung-Chi, C. and W.H. Prusoff, *Relationship between the inhibition constant (KI) and the concentration of inhibitor which causes 50 per cent inhibition (I50) of an enzymatic reaction.* Biochemical Pharmacology, 1973. **22**(23): p. 3099-3108.